

10.1071/FP17323\_AC

CSIRO 2018

Supplementary Material: *Functional Plant Biology*, 2018, 45(10), 983–999.

## Supplementary Material

### **Diversity in structure and forms of carbon assimilation in photosynthetic organs in *Cleome* (Cleomaceae)**

*Elena V. Voznesenskaya*<sup>A</sup>, *Nuria K. Koteyeva*<sup>A</sup>, *Asaph Cousins*<sup>B</sup> and *Gerald E. Edwards*<sup>B,C</sup>

<sup>A</sup>Laboratory of Anatomy and Morphology, Komarov Botanical Institute of the Russian Academy of Sciences, St Petersburg, Russia.

<sup>B</sup>School of Biological Sciences, Washington State University, Pullman, WA 99164-4236, USA.

<sup>C</sup>Corresponding author. Email: edwardsg@wsu.edu

**Table S1. Source of seeds and voucher specimen reference**

Species	Source of seeds	Origin of seeds	Voucher specimens
<i>C. africana</i> Botsch.	Royal Botanic Gardens, Kew, #0142768	Egypt <sup>a</sup>	Marion Ownbey Herbarium, Washington State University, WS 369771
<i>C. gynandra</i> L.	Originally provided by Dr. A.S. Raghavendra	Hyderabad, India <sup>b</sup>	Marion Ownbey Herbarium, Washington State University, WS 369765
<i>C. angustifolia</i> Forssk.	Herbarium material provided by Drs. A. Oskolskii and O. Maurin	Kruger National Park, Kruger, South Africa <sup>c</sup>	Marion Ownbey Herbarium, Washington State University, WS 375818
<i>C. paradoxa</i> R. Br. ex DC.	Royal Botanic Gardens, Kew, #0109051	Yemen <sup>d</sup>	Marion Ownbey Herbarium, Washington State University, WS 369807

<sup>a</sup>It occurs throughout northern Africa and the Arabian Peninsula, to Egypt, Israel, Jordan and Iraq (Kamel *et al.* 2010).

Distribution includes growth in moist sandy saline depressions and fine textured deep soils.

[http://uses.plantnet-project.org/en/Cleome\\_amblyocarpa\\_\(PROTA\)](http://uses.plantnet-project.org/en/Cleome_amblyocarpa_(PROTA)).

Kamel WM, Abd El-Ghani MM, El-Bouce MM (2010) Cleomaceae as a distinct family in the flora of Egypt. *The African Journal of Plant Science and Biotechnology* **4**, 11–16.

<sup>b</sup>In Hyderabad plants germinate just after the wet monsoon in June (mean high temperature 35°C), and terminate their life cycle in November (mean high temperature 29°C), with decreasing rainfall during the growing season (Dr. Raghavendra, personal communication; <https://www.google.com/search?q=annual+temperatures+hyderabad>).

<sup>c</sup>The park has mountains, bush plains and tropical forests; the mean high monthly temperature is 26°–32°C; see <http://www.holiday-weather.com/kruger/averages/> and <https://www.sanparks.org/parks/kruger/default.php/>. It occurs in mountainous, arid to semi-arid regions; in dry woodlands or bushlands, sometimes as a weed in cultivated areas. It is widely distributed in areas of tropical Africa with an annual rainfall of less than 500 mm. ([http://uses.plantnet-project.org/e/index.php?title=Cleome\\_angustifolia\\_\(PROTA\)&redirect=no](http://uses.plantnet-project.org/e/index.php?title=Cleome_angustifolia_(PROTA)&redirect=no)).

<sup>d</sup>An African species growing in semi-desert areas. *Cleome paradoxa* from the RBGE herbarium collection (E00375026) was collected in Aden, Yemen (<http://data.rbge.org.uk/herb/E00375026>). Aden has a hot desert climate; the annual average temperature in Aden is 29.2°C with average monthly temperatures variation of 7°C. <https://en.wikipedia.org/wiki/Aden#Climate>

## Supplementary methods

### *Western blot analysis*

Soluble proteins were extracted from different plant organs (cotyledons, leaves, petioles, stems and pod walls) by homogenizing 0.2 g of tissue frozen in liquid N<sub>2</sub> with 0.2 mL of extraction buffer [100 mM Tris-HCl, pH 7.5, 10 mM (w/v) MgCl<sub>2</sub>, 1 mM (w/v) EDTA, 15 mM (v/v) β-mercaptoethanol, 20 % (v/v) glycerol, and 1 mM phenylmethylsulfonyl fluoride]. After centrifugation at 10 000g for 10 min in a microcentrifuge, the supernatant was diluted 1:1 in [60 mM Tris-HCl, pH 7.5, containing 4 % (w/v) SDS, 20 % (v/v) glycerol, 1% (v/v) β-mercaptoethanol, and 0.1 % (w/v) bromphenol blue] and boiled for 5 min for analysis by SDS-PAGE. Protein concentration was determined with an RCDC protein quantification kit (Bio-Rad). Protein samples (20 µg) were separated by 10 % SDS-PAGE (see Fig. S1, for a loading control), blotted onto nitrocellulose, and probed overnight at 4°C with anti-*Amaranthus hypochondriacus* NAD-ME IgG which was prepared against the 65 KDa α subunit, courtesy of J. Berry (Long and Berry 1996) (1 : 2000), anti-*Zea mays* PEPC IgG (Chemicon, Temecula, CA, USA) (1 : 20000), anti-*Zea mays* pyruvate, Pi dikinase (PPDK) IgG, courtesy of T. Sugiyama (1 : 20000), anti-*Nicotiana tabacum* Rubisco (large subunit) IgG, courtesy of R. Chollet (1 : 10000). Goat anti-rabbit IgG-alkaline phosphatase conjugate antibody (Sigma) was used at a dilution of 1 : 10000 for detection. Bound antibodies were localized by developing the blots with 20 mM nitroblue tetrazolium and 75 mM 5-bromo-4-chloro-3-indolyl phosphate in detection buffer (100 mM Tris-HCl, pH 9.5, 100 mM NaCl, 5 mM MgCl<sub>2</sub>). The intensities of bands in western blots in the different organs were quantified using the ImageJ 1.37 program, and expressed relative to level in the leaves.

### *In situ immunolocalisation*

Plant samples were fixed at 4°C in 2% (v/v) paraformaldehyde and 1.25% (v/v) glutaraldehyde in 0.05 M PIPES buffer, pH 7.2. The samples were dehydrated with a graded ethanol series and embedded in London Resin White (LR White, Electron Microscopy Sciences, Fort Washington, PA, USA) acrylic resin. Antibodies used (all raised in rabbit) were anti-*Nicotiana tabacum* Rubisco (large subunit) IgG, courtesy of R. Chollet, commercially available anti-*Zea mays* L. PEPC IgG (Chemicon, Temecula, CA, USA) and anti-pea mitochondrial P-subunit of glycine decarboxylase IgG (courtesy of D. Oliver). Preimmune serum was used in all cases for controls.

To access the compartmentation of PEPC and Rubisco, leaf, petiole and stem cross sections, 0.8 to 1 µm thick, were dried from a drop of water onto gelatin coated slides and blocked for 1 h with TBST + BSA (10 mM Tris-HCl, 150 mM NaCl, 0.1% v/v Tween 20, 1% w/v BSA, pH 7.2). They were then incubated for 3 h with either

preimmune serum diluted in TBST + BSA (1 : 100 dilution), anti-Rubisco (1 : 50), or anti-PEPC (1 : 200). The slides were washed with TBST + BSA and then treated for 1 h with 10 nm protein A-gold particles (diluted 1 : 100 with TBST + BSA). After washing, the sections were exposed to a silver enhancement reagent for 20 min according to the manufacturer's directions (Amersham, Arlington Heights, IL, USA), stained with 0.5% (w/v) Safranin O, and imaged in a reflected/transmitted mode using a Zeiss Confocal LSM 510 Meta Laser Scanning Microscope (Carl Zeiss, Inc. Headquarters, Thornwood, NY). The background labeling with preimmune serum was very low, although occasional labeling occurred in areas where the sections were wrinkled due to trapping of antibodies/label (results not shown).

To assess the compartmentation of GDC, transmission electron microscopy immunolabeling was performed using the anti-P protein of GDC antibody. Thin cross sections of different organs (petiole, stem, or pod walls), on formvar-coated nickel grids were incubated for 1 h in TBST + BSA to block non-specific protein binding on the sections. They were then incubated for 3 h with either the preimmune serum diluted in TBST + BSA (1 : 50) or anti-P protein of GDC (1 : 10) antibody. After washing with TBST + BSA, the sections were incubated for 1 h with Protein A-gold (15 nm) diluted 1 : 100 with TBST + BSA. The sections were washed sequentially with TBST + BSA, TBST, and distilled water, and then post-stained with a 1 : 4 dilution of 1% (w/v) potassium permanganate and 2% (w/v) uranyl acetate. Images were collected using a Hitachi H-600 and FEI Tecnai G2 transmission electron microscopes. The density of labeling was determined by counting the gold particles on electron micrographs and calculating the number per unit area ( $\mu\text{m}^2$ ) with an image analysis program ImageJ 1.37. For each cell type, replicate measurements were made on parts of cell sections ( $n = 10$  to 15). The difference in labeling intensity between cell types is shown for each species. Since immunolabeling procedures were performed separately for each species, there is not an absolute quantitative estimate of differences between species. The level of background labeling was low in all cases.

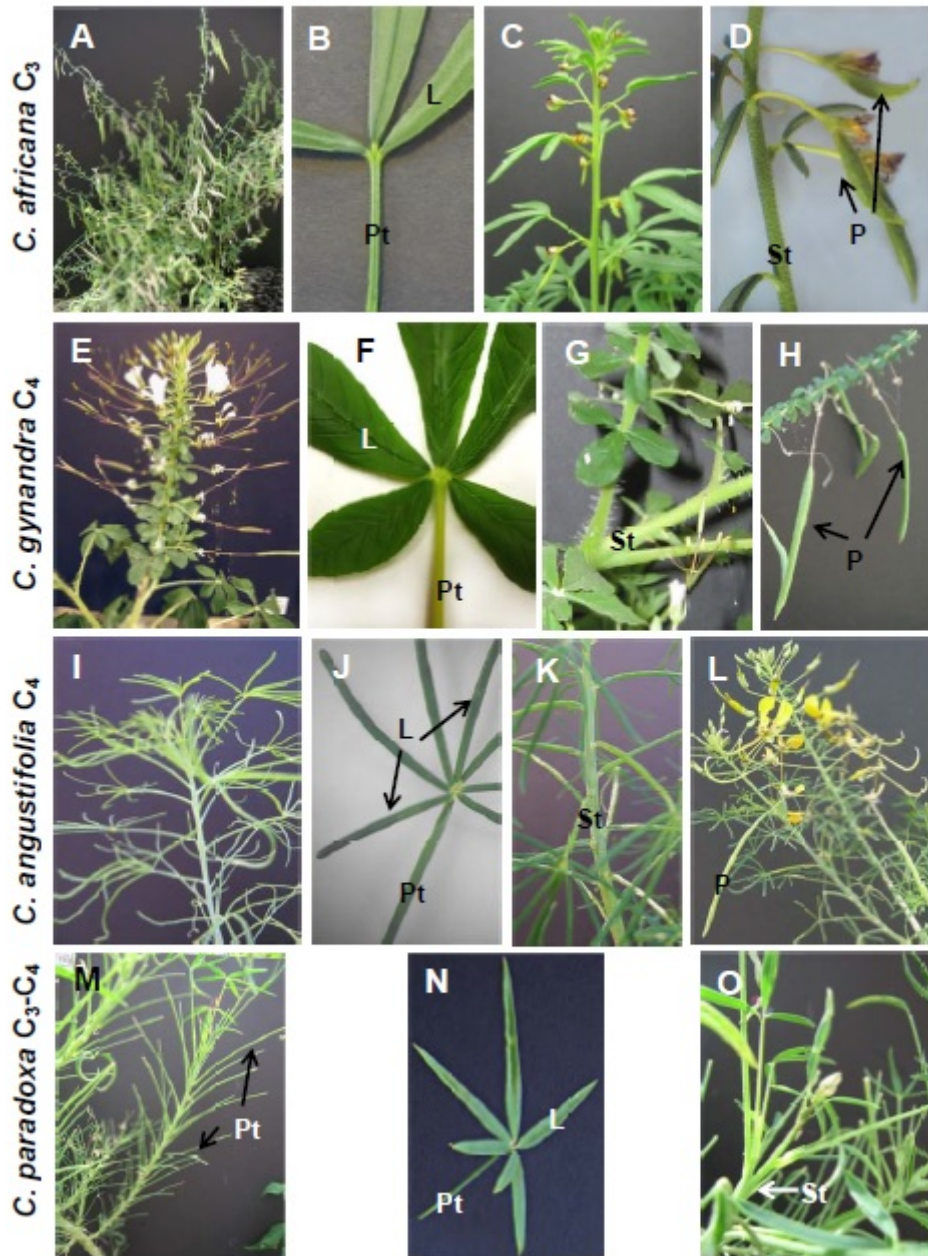


**Fig. S1.** General view of different organs in four *Cleome* species having different forms of photosynthesis in leaves (*C. africana* C<sub>3</sub>, *C. gynandra* C<sub>4</sub>, *C. angustifolia* C<sub>4</sub>, and *C. paradoxa* C<sub>3</sub>-C<sub>4</sub>). General view of plants (A, E, I, M). Leaves with petioles (B, F, J, N). Stems (C, D, G, K, O). Pods (D, H, L). Pods did not develop in *C. paradoxa* (O). L, leaflets; P, pod; Pt, petiole; S, stem.

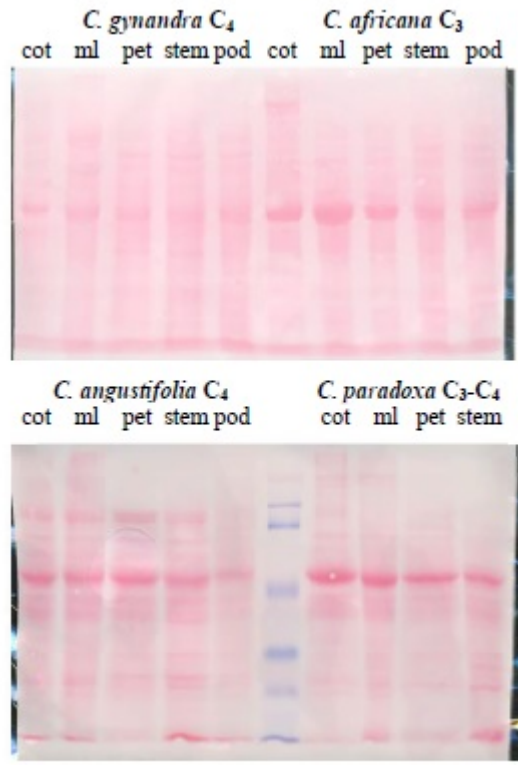


**Fig. S2.** Representative membranes stained with Ponceau S after proteins (20  $\mu$ g per lane) were transferred to nitrocellulose membrane and before immunoblotting. Cot, cotyledon; ml, mature leaf; pet, petiole.

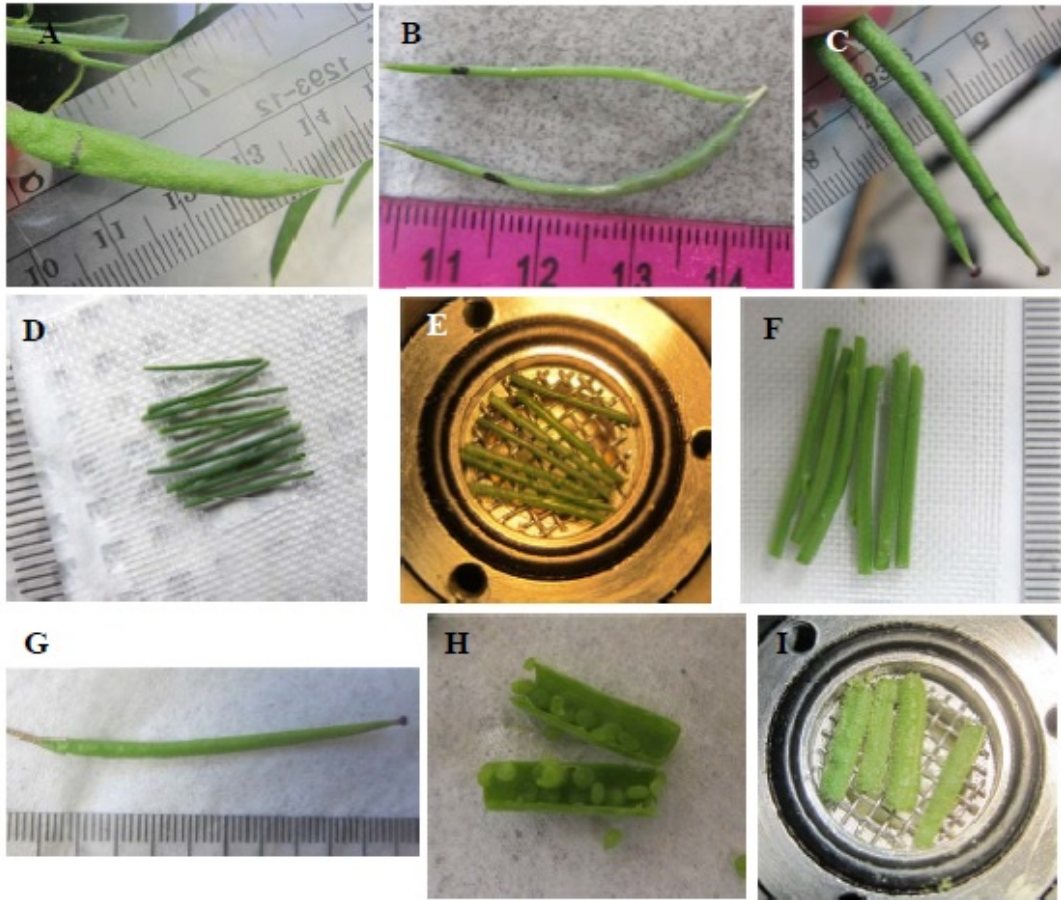


**Fig. S3.** Images of different organs used for gas exchange measurements by LiCor gas exchange system and inlet mass-spectrometry. (A–C) Intact pods used for gas exchange measurements by LiCor, *C. africana* (A), *C. angustifolia* (B), and *C. gynandra* (C). (D–F) Excised *C. angustifolia* petioles (D, E) and *C. africana* stems (F) used for gas exchange measurements by LiCor (D, F) and inlet mass-spectrometry (E). (G–I) Excised *C. gynandra* pod (G), removing the seeds (H), and appearance of pod walls in the chamber for inlet mass-spectrometric measurements (I).



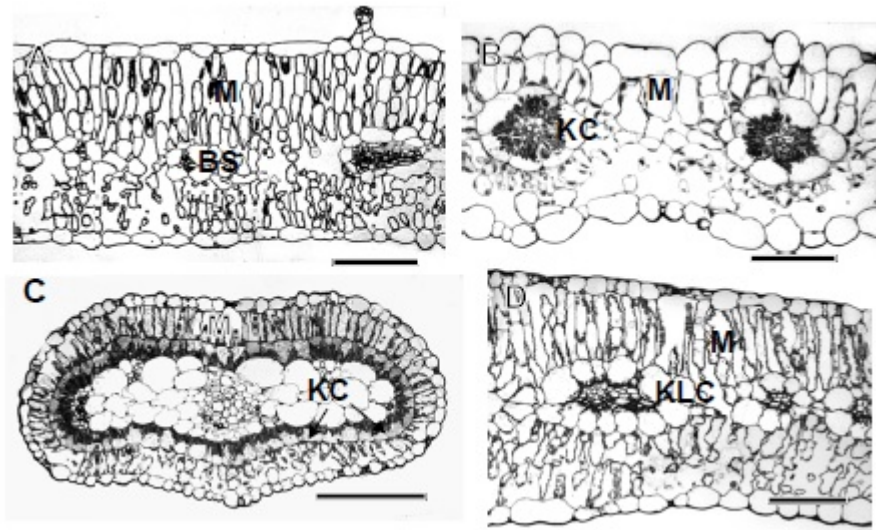


**Fig. S4.** General anatomy in leaves of *Cleome africana* (A), *C. gynandra* (B), *C. angustifolia* (C), *C. paradoxa* (D). BS, bundle sheath cells; KC, Kranz cells; KLC, Kranz-like cells; M, mesophyll cells. Scale bars: 200  $\mu\text{m}$  for A, 100  $\mu\text{m}$  for B–D. Leaves of *C. africana* are dorsoventral, with 3 chlorenchymatous palisade mesophyll (M) layers on the adaxial side and 3 layers of spongy M parenchyma on the abaxial side. *C. gynandra* has leaves with Atriplicoid anatomy with layers of Kranz cells (KC) and M cells surrounding each vascular bundle (VB). The  $\text{C}_4$  species *C. angustifolia* has terete leaves of Glossocardioid type of anatomy with two continuous layers of chlorenchyma, M and KC, located on the leaf periphery, with water storage tissue in the center of the leaf. In the  $\text{C}_3$ - $\text{C}_4$  intermediate *C. paradoxa* leaves are isopalisade, with two layers of palisade M chlorenchyma on both sides of the leaf and VBs located in the middle part of the leaf surrounded by well-developed Kranz-like cells (KLC) (=Kranz-like BS). *C. africana* has the thickest leaves (1.4 times thicker than *C. paradoxa*, twice as thick as leaves of *C. gynandra* and about 3 times thicker than terete leaves of *C. angustifolia*). All species are amphistomatic, with stomates distributed on the both sides of the leaves with a similar frequency except for *C. angustifolia* having more stomata on the adaxial leaf surface (Table 2).

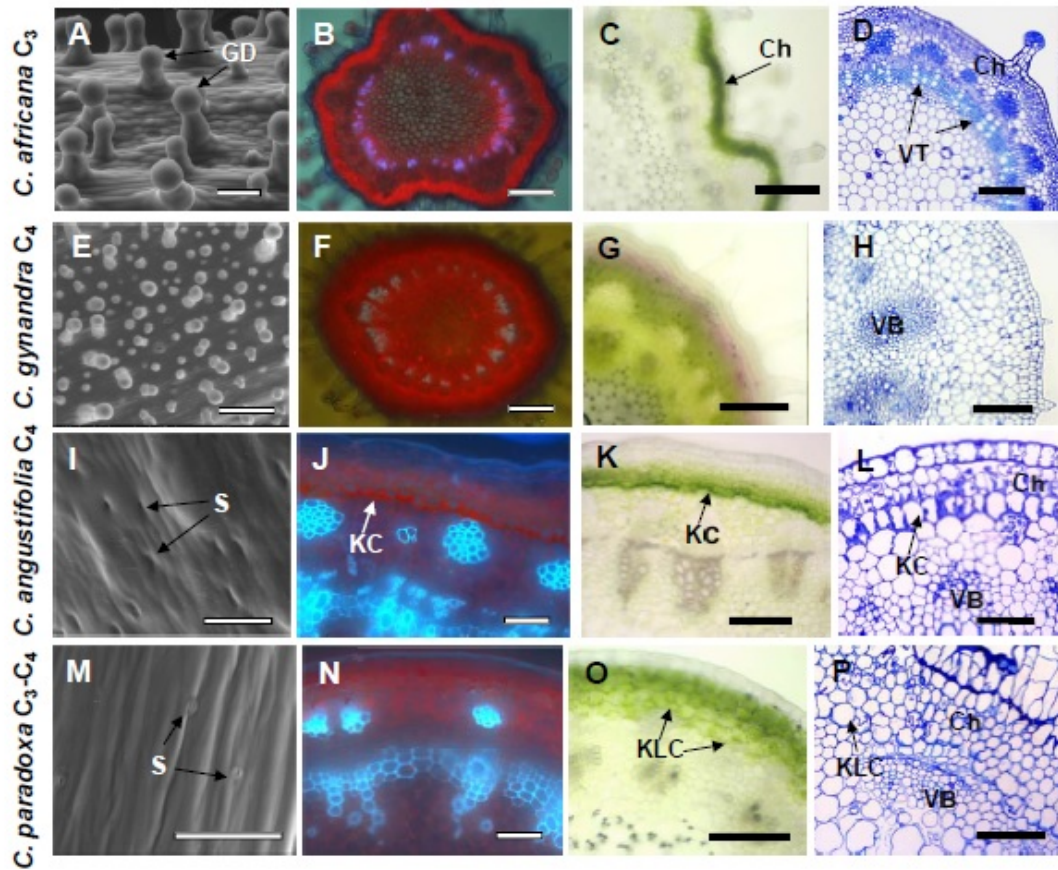


**Fig. S5.** Microscopy of stems of four *Cleome* species that have different types of photosynthesis in leaves. Outer surface of young stems showing glandular trichomes and stomata (A, E, I, M), the distribution of chlorenchyma (shown in red color) in cross sections under UV-light (B, F, J, N), sections of fresh stems, green color shows distribution of chloroplasts (C, G, K, O) and light microscopy of cross sections of stems. (D, H, L, P) *C. africana*, (A–D) *C. gynandra*, (E–H) *C. angustifolia*, (I–L) *C. paradoxa* (M–P). Ch, cortical chlorenchyma; GT, glandular trichomes; KC, Kranz cells; KLC, Kranz-like cells; S, stomates; VB, vascular bundles; VT, vascular tissue. Scale bars = 200  $\mu\text{m}$  for A–C, G, I–K, M, O; 100  $\mu\text{m}$  for D–F, H, L, N, P.

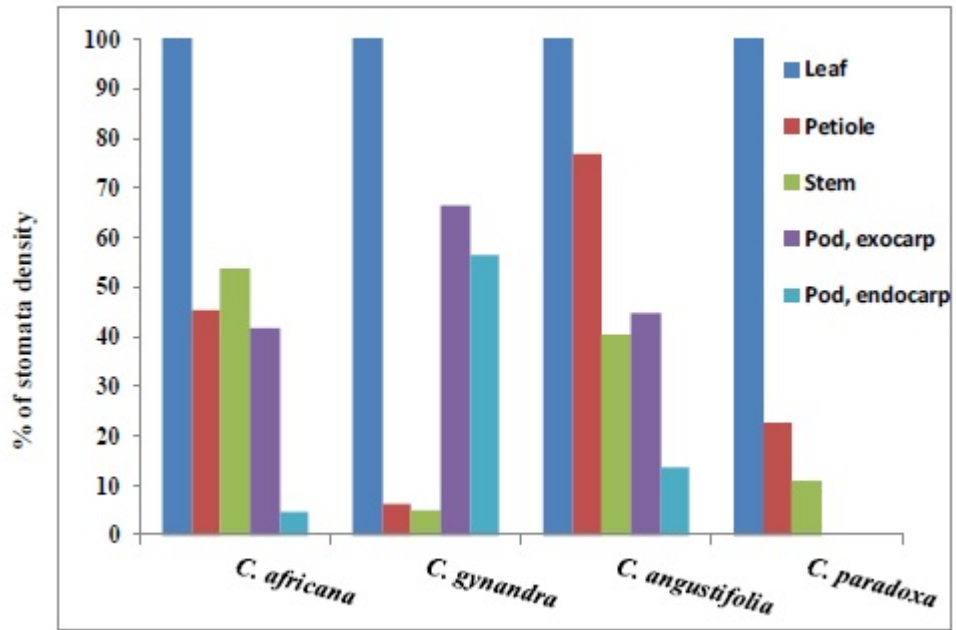


**Fig. S6.** The percentage of stomata density (%) for different organs relative to that in leaves (100%) of four *Cleome* species.

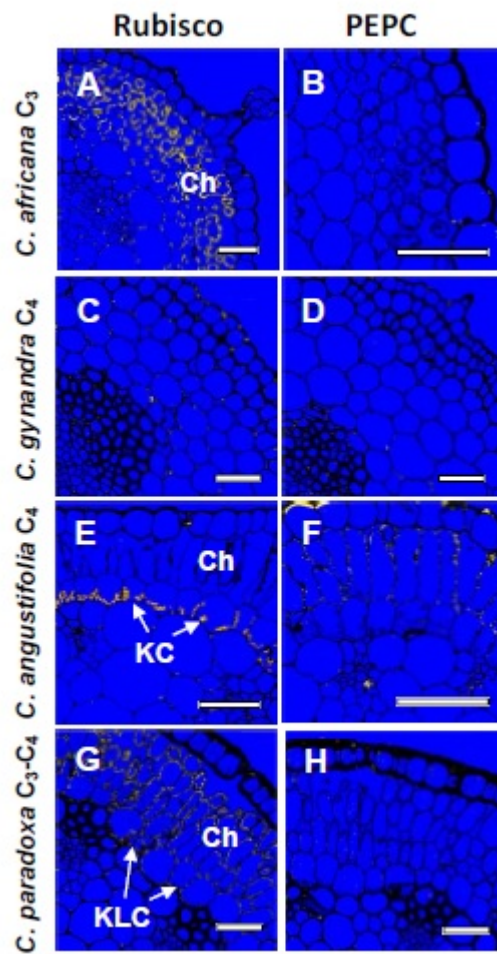


**Fig. S7.** *In situ* immunolocalization for Rubisco using antibody to the large subunit (A, C, E, G) and PEPC (B, D, F, H) in cross sections of petioles of *Cleome africana* C<sub>3</sub> (A, B), *C. gynandra* C<sub>4</sub> (C, D), *C. angustifolia* C<sub>4</sub> (E, F) and *C. paradoxa* C<sub>3</sub>-C<sub>4</sub> (G, H). Ch, chlorenchyma; KC, Kranz cells; KLC, Kranz-like cells. Scale bars: 50 μm for (A–H).

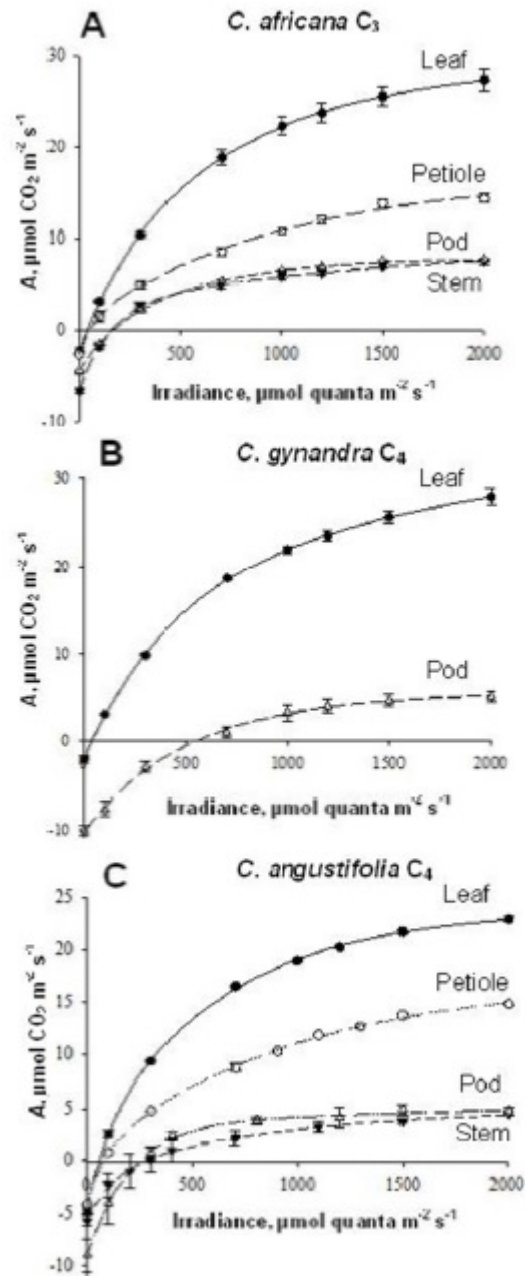


**Fig. S8.** Light response curves for selected photosynthetic organs of *C. africana* C<sub>3</sub>, *C. gynandra* C<sub>4</sub>, and *C. angustifolia* C<sub>4</sub>. Mature leaves (closed circles), petioles (open circles), stems (open triangles), pods (closed triangles).

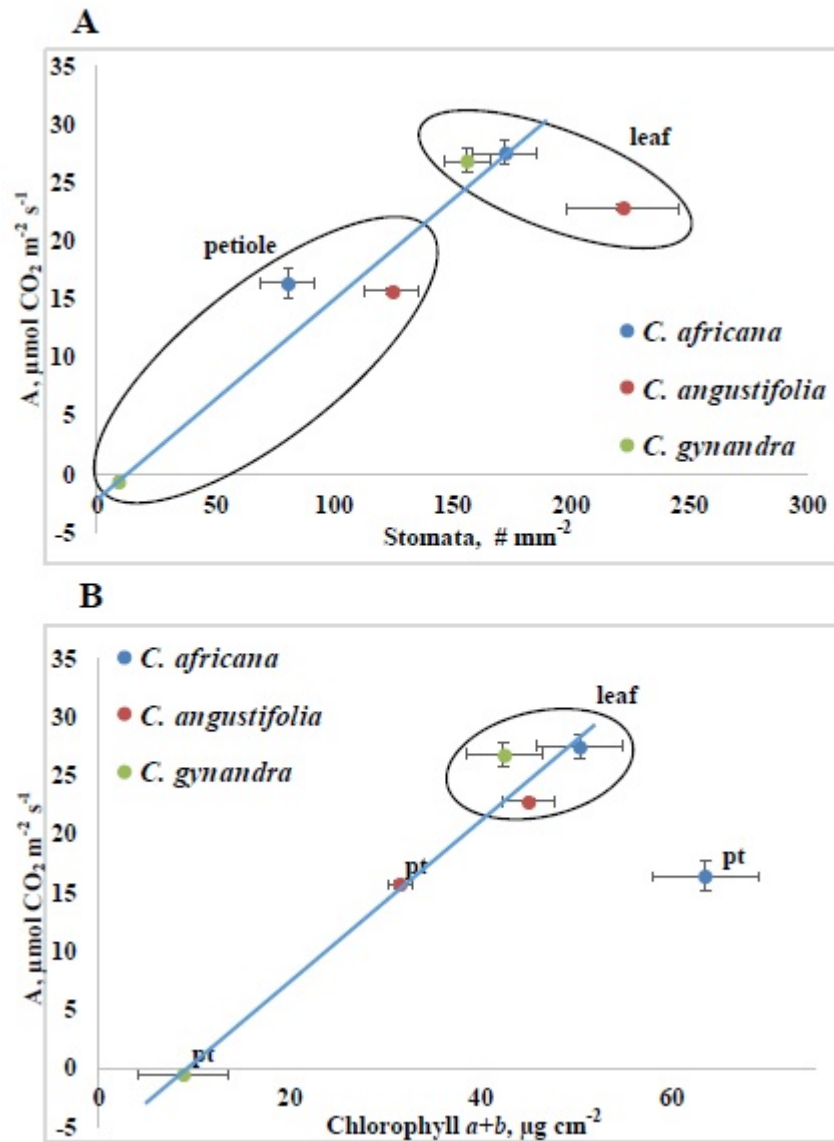


**Fig. S9.** Rates of photosynthesis (A) per projected area (at 2000 PPFD, 400 ppm CO<sub>2</sub> and 25°C) versus stomata number per area (average of adaxial and abaxial) (A) and versus chlorophyll *a+b* content per area (B) measured on leaves and petioles of *C. africana* C<sub>3</sub>, *C. gynandra* C<sub>4</sub>, and *C. angustifolia* C<sub>4</sub>. Each point is a mean of 2–3 separate measurements. pt, petiole.